






## The change of the domain wall shape under the ion beam irradiation in lithium niobate

Elena Pashnina , Alla Slautina , Andrey Akhmatkhanov \*,  
Maria Chuvakova  and Vladimir Shur   
*School of Natural Sciences and Mathematics  
Ural Federal University, Ekaterinburg 620002, Russia  
\*andrey.akhmatkhanov@urfu.ru*

Received 10 April 2024; Revised 23 May 2024; Accepted 11 June 2024; Published 10 July 2024

In this paper, we present the study of the shape change on the polar surface and in the bulk of the walls of lamellar domains as a result of local switching by focused ion beam. Periodical lamellar domain structures (PDS) are created alternatively by two methods: (i) electric-field poling using photolithographically defined electrodes and (ii) ion beam poling. The dot irradiation of  $Z^+$  areas near the walls of lamellar domains leads to the formation of faceted or rounded hexagonal domains. For e-field PDS additional formation of nanodomain ensembles was observed. We have revealed two types of domain wall shape changes induced by irradiation: (1) merging of the hexagonal domain with the domain wall for  $Z^+$  areas; (2) formation of rounded distortion of the domain wall for  $Z^-$  areas. For  $Z^+$  areas irradiation, the domain wall distortion was described by a simple model of independent growth of isolated domain with its subsequent merging with a static domain wall. For  $Z^-$  surface irradiation, the domain wall shift increases linearly with the distance between the irradiation dot and the wall. It was revealed that the merging between the growing hexagonal pyramid domain and lamellar domain can be obtained in the bulk even for absence of merging at the surface. All obtained results have been explained within a kinetic approach to the domain wall motion by step generation. The switching field consists of inputs produced by: (i) the charges injected during dot irradiation into the photoresist layer and crystal bulk, (ii) the charges injected during the creation of i-beam PDS, (iii) the depolarization fields. The transition of the shapes of isolated domains and wall distortions from faceted to rounded ones with field increase was attributed to the transition from determined step generation to stochastic one.

**Keywords:** Domain structure; ion beam irradiation; screening; domain kinetics; periodical poling.

### 1. Introduction

Lithium niobate (LN,  $\text{LiNbO}_3$ ) single crystals with tailored periodical domain structures (PDS) have emerged as one of the key platforms for enabling various types of laser wavelength nonlinear conversion processes.<sup>1,2</sup> Periodically poled LN crystals (PPLN) with proper period provide a strong increase in the efficiency of the nonlinear optical conversion process due to the realization of the quasi-phase matching.<sup>3,4</sup> Significant advances in domain engineering methods for the creation of PDS stimulated the search for new applications of tailored domain structures in other fields beyond nonlinear optics.<sup>5,6</sup> One of these emerging fields is ferroelectric lithography — the technique of creation of artificial patterns on the surface of ferroelectric crystal by selective deposition of material on domains of different signs or domain walls.<sup>7</sup> Ferroelectric lithography is based on different photochemical surface reactivity of different domains/domain walls or uncompensated electric field appearing in the vicinity of domain walls. During the last decades, this approach has evolved from relatively simple photochemical deposition of metallic nanoparticles<sup>8–19</sup> to deposition of dielectric nanostructures,<sup>20–23</sup> organic molecules<sup>24</sup> and even biological

objects.<sup>5</sup> As the ferroelectric template in this case can be potentially used for replication of large number of functional patterns, the problem of correction of the initially created domain structure arises. This problem is analogous to the photomask correction by ion beam techniques for conventional photolithography.

From the fundamental point of view, the problem is related to the studies of domain wall shape change induced by local polarization reversal in the vicinity of this wall. This process was studied previously in congruent PPLN single crystals during local polarization reversal by biased or grounded conductive tip of scanning probe microscope (SPM).<sup>25</sup> In that paper, the authors demonstrated that scanning by grounded SPM tip across the plane macroscopic domain wall leads to the appearance of nanodomains near the wall and nanometer-scale perturbations on the wall. At the same time, the change of domain wall shape as a result of field application by a stationary biased SPM tip was not studied in detail. The change of the domain wall shape in the bulk was not studied in the mentioned paper as well, while it is known that the domain structure evolution on the polar surface is strongly influenced by the domain shape in the bulk.<sup>26</sup>

The most widely used technique for the creation of tailored domain structures is electric-field poling by means of the photolithographically defined electrodes (e-field poling).<sup>2</sup> Moreover, it was demonstrated that the local irradiation by a focused electron beam or ion beam (e-beam or i-beam poling) allows to produce the PDS in bulk crystals.<sup>27–30</sup> E-field poling is the most widespread technique of PPLN creation providing domain structure periods down to a few microns<sup>2</sup> and potentially ready for mass production. I-beam poling at the same time provides the possibility for the creation of even finer structures<sup>31</sup> and can be applied for proof-of-concept projects and small-volume production. Therefore, it is important to study the possibilities of correction of domain structure created by both these methods.

It is known that the domain structure evolution during polarization reversal is strongly influenced by a screening process of the depolarization field.<sup>32,33</sup> From this point of view, the difference in studying the domain structure evolution during local switching near domain structures created by e-field and i-beam poling techniques consists in the degree of depolarization field compensation. In our experiments, the tailored domain structure created by e-field poling is locally switched a long time after its creation (more than 6 months) while the one created by i-beam poling is switched in 3 s after creation which is comparable to characteristic times of bulk screening processes in congruent LN.<sup>34</sup> It means that the depolarization field will be almost fully compensated for e-field poling and only partially compensated for i-beam poling.

In this paper, we present the study of the shape change on the polar surface and in the bulk of the plane wall as a result of local switching by the ion beam. The initial domain structure representing periodical lamellar domains is created by e-field and i-beam poling techniques.

## 2. Materials and Methods

In this work, we have used an array of stripe domains aligned along  $Y$  crystallographic axis as a model-tailored domain

structure. The PDS was created in 500  $\mu\text{m}$  thick congruent Z-cut LN (Crystal Tech., USA) samples. Two types of tailored domain structures were studied: (1) e-field PDS produced by e-field poling and (2) i-beam PDS produced by i-beam poling.

For e-field poling, a periodic electrode pattern was created by photolithography using photoresist AZ ECI 3027 (AZ Microchemicals, Germany) with a thickness of 3.8  $\mu\text{m}$ . A system of periodical stripe windows in the photoresist layer with a width of 6  $\mu\text{m}$  and a period of 15  $\mu\text{m}$  was created on Z<sup>+</sup> polar surface and heat treatment at 130°C was carried out to increase the stability of the photoresist. The polar surfaces were covered with liquid electrolytes (saturated aqueous solution of LiCl). The PDS was created by application of field pulses with amplitude ranging from 21.5 to 21.8 kV/mm and duration from 100 to 300 ms. As a result, the through PDS with a 15  $\mu\text{m}$  period was created (Fig. 1(a)). The photoresist was removed before dot i-beam irradiation.

For i-beam poling, the Z<sup>+</sup> surface of the sample was uniformly covered by photoresist layer AZ nLOF 1505 with a thickness of 0.5  $\mu\text{m}$  for charge localization.<sup>30,35</sup> On the opposite polar surface, a solid copper electrode was deposited by the magnetron sputtering. The electrode was grounded during irradiation. The dual beam workstation Auriga CrossBeam (Carl Zeiss, Germany) equipped with a field emission gun, and a ion beam with a liquid-metal Ga ion source was used for domain switching. An electron–ion beam lithography system Raith MultiBeam (Raith, Germany) made it possible to control the beam movement and its parameters. The irradiation pattern represented the periodical stripes realized by a raster scan with a period of 18  $\mu\text{m}$  and a width of 4.5  $\mu\text{m}$ . The following irradiation parameters were chosen: a dose of 400  $\mu\text{C}/\text{cm}^2$ , an accelerating voltage of 30 kV and an ion beam current of 240 pA.

The created lamellar domain structures were imaged in bulk by Čerenkov-type second harmonics generation microscopy (SHGM) using the modified experimental setup based on NanoLaboratory NTEGRA Spectra (NT-MDT, Russia) (Fig. 1), and their main geometrical parameters were extracted (Table 1). SHGM is a nondestructive technique that

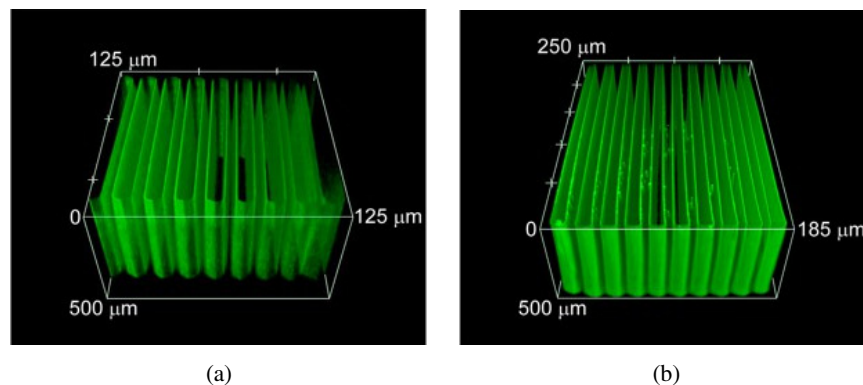


Fig. 1. SHGM 3D images of (a) e-field PDS and (b) i-beam PDS.

Table 1. Geometric parameters of the model PDS created by e-field and i-beam techniques. The measurement errors correspond to the resolution of SHGM.

Type of the structure	Period, $\mu\text{m}$	Stripe width on $Z^+$ , $\mu\text{m}$	Stripe width on $Z^-$ , $\mu\text{m}$	Duty cycle
E-field PDS	$15.0 \pm 0.3$	$9.5 \pm 0.2$	$10.1 \pm 0.9$	$0.65 \pm 0.02$
I-beam PDS	$18.2 \pm 0.3$	$9.4 \pm 0.4$	$9.9 \pm 0.5$	$0.53 \pm 0.02$

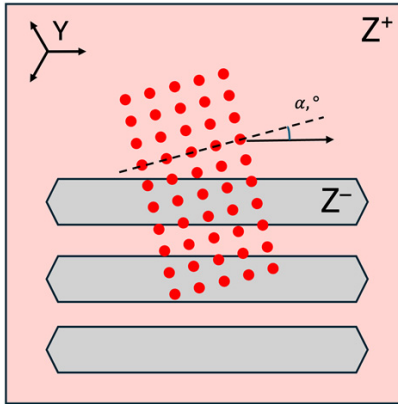


Fig. 2. Scheme of dot irradiation performed near the PDS.

can image domain walls at the bulk of the ferroelectric crystal.<sup>36,37</sup>

The isolated domains were created by dot irradiation. The doses of dot irradiation ranged from 1 to 10 pC. Several  $5 \times 14$  arrays of isolated domains with a  $4 \mu\text{m}$  period were created near the domain walls of PDS with the angle  $\alpha$  between array rows and  $Y$  crystallographic axis equal to  $0^\circ$ ,  $5^\circ$  and  $15^\circ$  (Fig. 2). The parameters of the ion beam were the same as for the creation of i-beam PDS.

The switching conditions for e-field and i-beam PDS were qualitatively different. For e-field PDS the photoresist layer was removed after periodical poling and the time interval between the PDS creation and dot irradiation was about several months, which is much longer than the characteristic time of depolarizing field screening in CLN. For i-beam PDS the dot irradiation occurred just after poling without removing of the photoresist layer with a time delay of about 3 s. In this case, the charge injected during i-beam poling remained in the photoresist layer.

After i-beam dot irradiation, the photoresist and bottom electrode were removed for domain imaging. The domain structures were imaged in the bulk by SHGM and on the polar surface after selective chemical etching by scanning electron (SEM) and ion (SIM) microscopy.

### 3. Results

#### 3.1. Formation of isolated domains

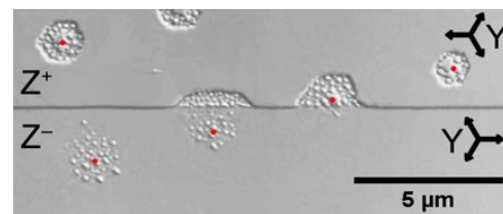
For the sample with e-field PDS, it was shown that the dot irradiation of  $Z^+$  areas leads to formation at the surface typical for LN hexagonal domains<sup>32</sup> covered by isolated

nanodomains with initial polarization direction (Fig. 3(a)). In contrast the dot irradiation of  $Z^-$  areas leads to the formation of the ensembles of nanodomains only (Fig. 3(a)). The nanodomain density in both cases was about  $0.5 \mu\text{m}^{-2}$ .

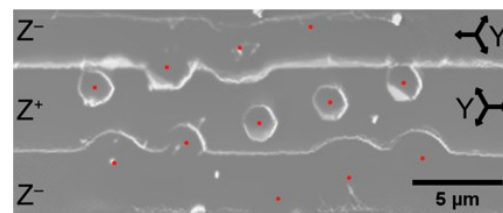
For i-beam PDS, the dot irradiation leads to formation at the surface of rounded hexagonal domains for irradiated  $Z^+$  areas only (Fig. 3(b)). The average domain size was about 1.4 times larger than that for samples with e-field PDS. This fact can be attributed to the action of the field produced by the injected charges during the creation of the i-beam PDS.

#### 3.2. Change of plane domain wall shape at the surface

The dot irradiation near the plane wall of the stripe domain changes its shape (Figs. 3 and 4(c)) for e-field and i-beam PDS. In both cases we distinguished two types of domain wall shape changes: (1) merging of the hexagonal domain with the domain wall for irradiation of  $Z^+$  surface; (2) formation of rounded bump (distortion) on the domain wall for irradiation of  $Z^-$  surface (Figs. 3 and 4(c)). We have analyzed the domain wall distortion in terms of the maximal displacement of the domain wall from its initial position ( $L$ ) as a function of the distance between the irradiation dot and the initial wall position ( $D$ ) (Fig. 4). Negative values of  $D$  correspond to the irradiation of  $Z^-$  polar surface, positive values



(a)



(b)

Fig. 3. (a) SEM and (b) SIM images of domains at the surface, formed as a result of dot irradiation in samples with (a) e-field PDS and (b) i-beam PDS. The dose is 10 pC. The red dots indicate the positions of the i-beam during dot irradiation.

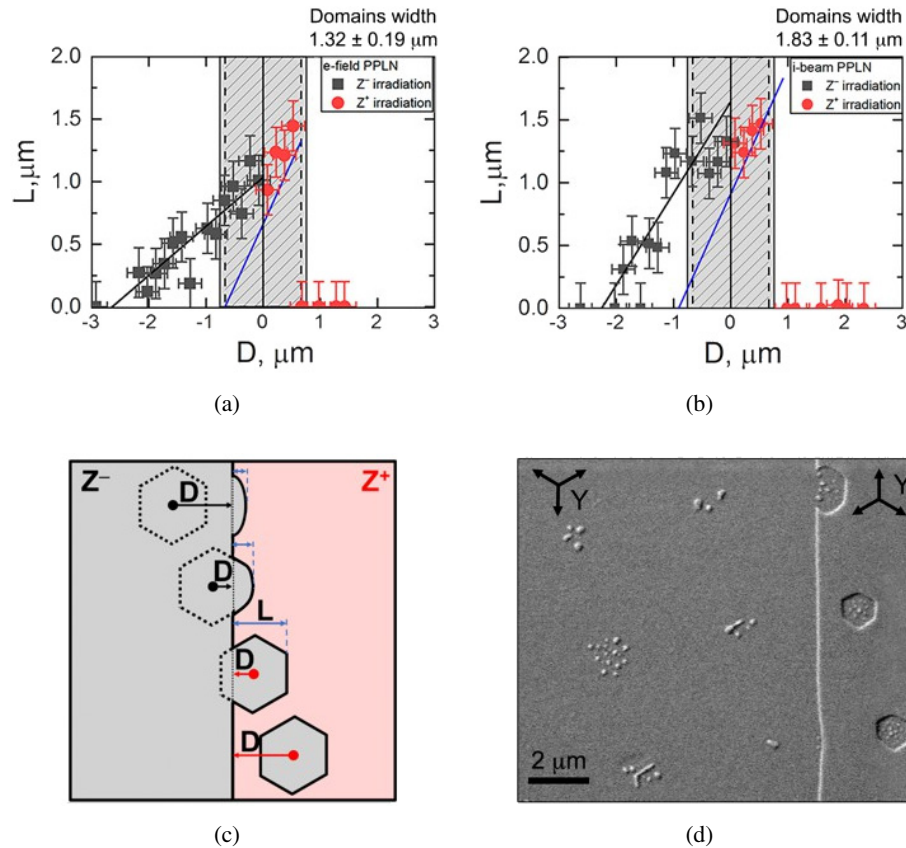


Fig. 4. (Color online) (a, b) Dependence of displacement of the wall of a stripe domain on the distance between the irradiation dot and the initial wall position in the samples with (a) e-field PDS and (b) i-beam PDS for irradiation dose 10 pC. The gray region on (a) and (b) corresponds to the size of the isolated domain. The black solid lines are linear approximations of the experimental data. The blue dotted line corresponds to complete absence of interaction between the stripe domain and the growing domain. (c) Scheme of the domain wall distortion during i-beam dot irradiation. (d) SEM image demonstrating the formation of concave angles during the merging of isolated domain and plane domain wall. The dose is 5 pC, e-field PDS.

correspond to the irradiation of  $Z^+$  polar surface (Figs. 4(a) and 4(b)).

For the case of  $Z^+$  surface irradiation, the domain wall distortion occurs only as a result of merging with the growing domain (Figs. 3, 4(a) and 4(b)). For irradiation distance  $D$  above the halfwidth of the isolated domain ( $R$ ), the noticeable distortion of the domain wall was not observed (Figs. 4(a) and 4(b)). The domain walls with concave angles appeared during the merging of the growing domain and the domain wall (Fig. 4(d)) was never obtained for the merging of growing domains in CLN.<sup>38</sup> The domain structure evolution, in this case, can be described by a simple model of independent growth of isolated domain with its subsequent merging with stationary domain wall (red dots and blue lines in Figs. 4(a) and 4(b)).

Dot irradiation of  $Z^-$  polar surfaces leads to a linear dependence of  $L$  on  $D$  (black dots in Figs. 4(a) and 4(b)). The distortion of the domain wall shape in this case differs qualitatively from the case of the  $Z^+$  surface: it becomes rounded (Fig. 3(b)) with only slight faceting for e-field PDS (Fig. 3(a)). It should be noted that the domain wall distortion

was observed for the distance between the irradiation dot and initial wall position above  $2 \mu\text{m}$  which is much higher than the isolated domain halfwidth for  $Z^+$  surface irradiation (660 nm and 920 nm for e-field and i-beam PDS, respectively).

### 3.3. Change of plane domain wall shape in the bulk

The merging of hexagonal pyramid domains with lamellar domains has been studied in the crystal bulk using domain structure imaging in the bulk (Fig. 5). It was revealed that the merging in the bulk was obtained even for the absence of merging at the surface. For example, for dose 10 pC the merging occurred in the bulk at the depth of about  $10 \mu\text{m}$  for the distance from the irradiated dot and the PDS below  $2 \mu\text{m}$  (Figs. 5(a)–(c)). The domain merging led to the rounded distortion on the domain wall (Figs. 5(d) and 5(e)).

We have also studied the influence of existing lamellar domains on the growth depth of isolated domains formed during dot irradiation. It is known, that for dot irradiation in matrix, the growth depth of central domains is considerably

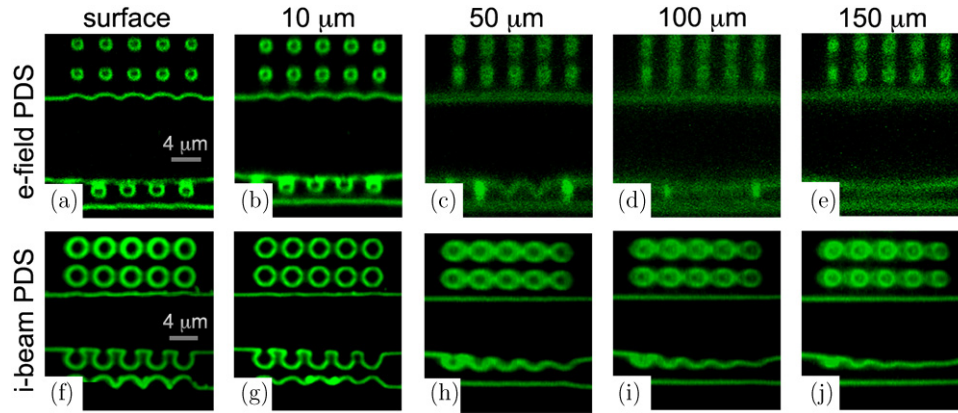


Fig. 5. SHGM images of the pyramid domains created near the wall of the lamellar domain obtained at different depths for (a–e) e-field PDS and (f–j) i-beam PDS. The dose is 10 pC.

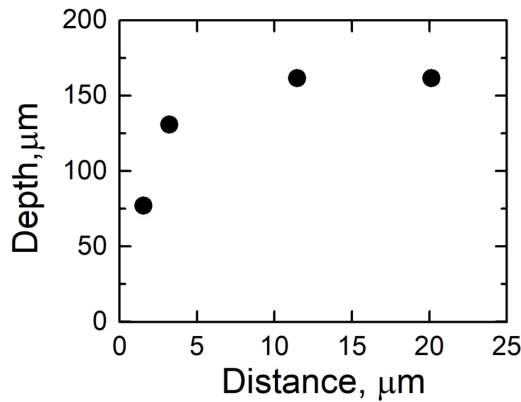


Fig. 6. Dependence of the depth of dot domains with the irradiation dose of 2 pC on the domain wall distance of the stripe domain in the i-beam PDS sample.

higher than that for peripheral ones.<sup>39</sup> To exclude this effect, we have analyzed the dependence of the growth depth on the distance from the wall of the lamellar domain for the isolated domains possessing the same coordinates (in the center) in a dot array (Fig. 6).

It was shown that the depth of isolated pyramid domains decreases by more than two times with a decrease in the distance between the irradiation dot and the plane domain wall of i-beam PDS (Fig. 6). For e-field PDS, this decrease is less pronounced.

#### 4. Discussion

For e-field PDS appearance of nanodomains as a result of dot irradiation can be attributed to the action of the field produced by charges injected in the crystal bulk. Domain growth in this case occurs under the action of the polar component of the switching field ( $E_{sw}$ ) which consists of the polar components of the fields produced by: (i) the charges injected into the photoresist layer ( $E_{inj}^{ph}$ ), (ii) the charges injected into crystal bulk ( $E_{inj}^b$ ) and (iii) the depolarization field ( $E_{dep}$ ). In the layer

near the surface,  $E_{inj}^{ph}$  and  $E_{inj}^b$  fields have opposite directions, thus

$$E_{sw} = E_{inj}^{ph} - E_{inj}^b - E_{dep}. \quad (1)$$

Just after ion beam irradiation the  $E_{inj}^{ph} \gg E_{inj}^b$  which leads to the growth of large hexagonal domains (Figs. 7(a) and 7(b)) for  $Z^+$  areas and absence of switching for  $Z^-$  areas (Figs. 7(d) and 7(e)).

The relaxation of the charge injected in the photoresist layer is much faster than in the crystal bulk. As a result of spatially nonuniform relaxation of the injected charge the switching field  $E_{sw}$  changes its direction (Figs. 7(c) and 7(f)). This fact leads to the formation of nanodomain ensembles in  $Z^-$  areas (Figs. 3(a), 7(c) and 7(f)). It is necessary to take in mind that  $Z^-$  areas appeared also in freshly switched domains for irradiation of  $Z^+$  areas (Fig. 7(b)). Therefore, the appeared large hexagonal domains are also covered by isolated nanodomains. The size and the shape of nanodomain ensembles are determined by the spatial distribution of the injected charges within the  $Z^-$  area (Figs. 7(c) and 7(f)). It should be noted that polarization reversal by the field produced by the charge injected in crystal bulk was studied previously during e-beam irradiation of CLN samples through a metal film.<sup>40–43</sup> In our case, most part of the injected charge is localized in the photoresist layer,<sup>30</sup> however, a few percent of injected charge reaching the crystal bulk is expected to be enough for nanodomain ensembles formation after relaxation of photoresist-injected charge.

For i-beam PDS the absence of nanodomains can be attributed to additional input in  $E_{sw}$  of the field produced by the charges injected into the photoresist during PDS creation ( $E_{inj}^{PDS}$ ). This input is co-directed with  $E_{inj}^{ph}$  and prevents nanodomain formation.

The rounded shape of isolated domains created for the dot irradiation of i-beam PDS only can be attributed to the higher value of the switching field as compared to e-field PDS due to additional input of  $E_{inj}^{PDS}$ . According to the kinetic approach step generation at the domain wall is proportional to the

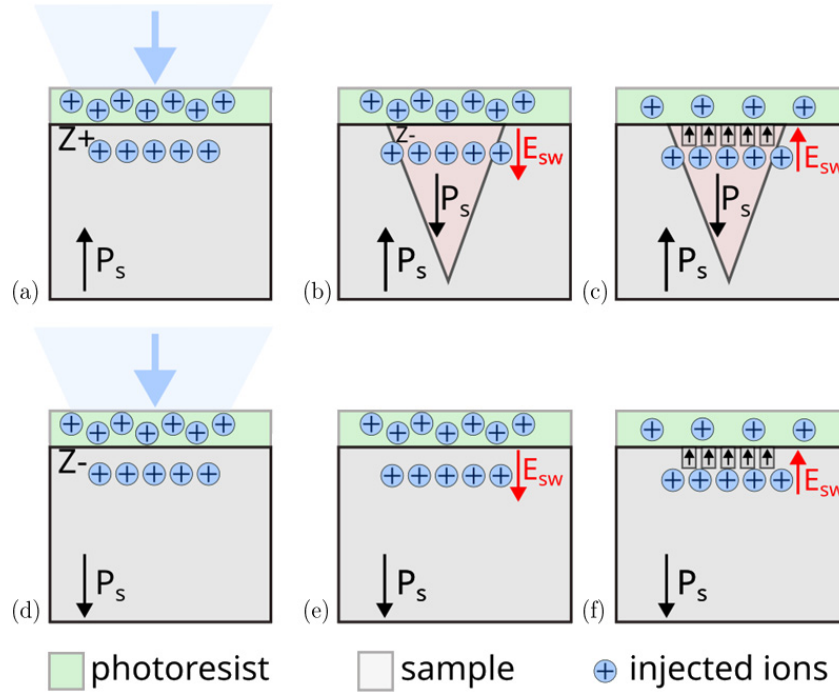


Fig. 7. Scheme of nanodomain formation after ion beam irradiation of polar areas: (a–c)  $Z^+$ , (d–f)  $Z^-$ . (a, b) Ion beam irradiation. (b) Formation of hexagonal pyramid domain. (c, f) Formation of nanodomains after injected charge relaxation in the photoresist layer.  $E_{sw}$  — total field produced by charges injected into photoresist and sample,  $E_{dep}$  — uncompensated depolarization field appeared after switching of hexagonal pyramid domain.

excess of the switching field over the threshold value.<sup>33</sup> The high enough value of the field excess leads to a transition to stochastic step generation and rounded domain shape.<sup>32</sup>

The different shapes of the wall's distortion of lamellar domains for irradiation of  $Z^+$  and  $Z^-$  areas can be explained in the same manner by different values of the switching field. For  $Z^-$  areas irradiation where the new isolated domain is not formed the depolarization field input  $E_{dep}$  (see Eq. (1)) is much lower and thus the switching field  $E_{sw}$  is much higher. This fact leads to the domination of the stochastic step generation with rounded wall distortion for  $Z^-$  areas and the determined step generation with faceted wall distortion for  $Z^+$  areas. The revealed merging of pyramidal and lamellar domains in the bulk is clear evidence of domain wall motion by step generation in the bulk under the action of the field produced by the array of the localized injected charges created by dot irradiation.<sup>39</sup>

The dependence of the depth of isolated pyramid domains on the distance between the irradiation dot and the plane domain wall for i-beam PDS can be attributed to the electrostatic interaction of charged walls of the formed pyramidal domains and lamellar domains. The fields produced by charged domain walls were not screened during the short time interval between the creation of i-beam PDS and the appearance of isolated domains. The effect is absent for e-field PDS with a complete screening of the fields.

## 5. Conclusion

We have studied the shape change of the plane walls of lamellar domains at the polar surface and in the bulk created by e-field and i-beam poling techniques as a result of local switching by ion beam.

It was shown that dot irradiation of  $Z^+$  areas near the lamellar domains of e-field PDS leads to the formation of the conventional hexagonal domains at the polar surface covered by isolated nanodomains with the initial polarization direction. In contrast the dot irradiation of  $Z^-$  areas leads to the formation of the nanodomain ensembles only. For i-beam PDS the dot irradiation leads to formation at the surface of rounded hexagonal domains for irradiated  $Z^+$  areas only.

We have revealed two types of domain wall shape changes induced by dot i-beam irradiation near them: (1) merging of the hexagonal domain with the domain wall for irradiation of  $Z^+$  areas; (2) formation of rounded distortion on the domain wall for irradiation of  $Z^-$  areas.

For  $Z^+$  areas irradiation, the domain wall distortion can be described by a simple model of independent growth of an isolated domain with its subsequent merging with a stationary domain wall.

For  $Z^-$  surface irradiation, the domain wall shift increases linearly with the distance between the irradiation dot and the domain wall. The wall distortion becomes rounded and was observed for the distances between the irradiation dot and

initial wall position considerably higher than the isolated domain halfwidth.

It was revealed that the merging between the growing hexagonal pyramid domain and the lamellar domain leading to the rounded distortion can be obtained in the bulk even for the absence of merging at the surface.

It was shown for i-beam PDS that the depth of isolated pyramid domains decreases by more than two times with a decrease in the distance between the irradiation dot and the plane domain wall.


All obtained results have been explained within a kinetic approach to the domain wall motion by step generation. The switching field consists of inputs produced by (i) the charges injected during dot irradiation into the photoresist layer and crystal bulk, (ii) the charges injected during the creation of i-beam PDS, (iii) the depolarization fields. The transition of the shapes of isolated domains and wall distortions from faceted to rounded is attributed to the higher values of the switching fields leading to a transition from determined step generation to stochastic one.


For practical applications, these results provide guidelines for correction of the created domain structure. It is shown that better correction accuracy (smaller feature size) is obtained when local switching is realized outside of the created domain (that is on  $Z^+$  surface).


## Acknowledgments

The research was made possible by the Russian Science Foundation (Project No. 21-72-10160). The equipment of the Ural Center for Shared Use “Modern nanotechnology” UrFU was used. We thank D. S. Chezganov for valuable comments.


## ORCID

Elena Pashnina  <https://orcid.org/0000-0002-8720-9178>

Alla Slautina  <https://orcid.org/0000-0002-1329-2474>

Andrey Akhmatkhanov  <https://orcid.org/0000-0002-2802-9134>

Maria Chuvakova  <https://orcid.org/0000-0002-3994-782X>

Vladimir Shur  <https://orcid.org/0000-0002-6970-7798>

## References

- 1 A. Boes, L. Chang, C. Langrock, M. Yu, M. Zhang, Q. Lin, M. Lončar, M. Fejer, J. Bowers and A. Mitchell, Lithium niobate photonics: Unlocking the electromagnetic spectrum, *Science* **379**, eabj4396 (2023).
- 2 V. Y. Shur, A. R. Akhmatkhanov and I. S. Baturin, Micro- and nano-domain engineering in lithium niobate, *Appl. Phys. Rev.* **2**, 040604 (2015).
- 3 J. A. Armstrong, N. Bloembergen, J. Ducuing and P. S. Pershan, Interactions between light waves in a nonlinear dielectric, *Phys. Rev.* **127**, 1918 (1962).
- 4 D. S. Hum and M. M. Fejer, Quasi-phases-matching, *C. R. Phys.* **8**, 180 (2006).
- 5 A. Blázquez-Castro, A. García-Cabañes and M. Carrascosa, Biological applications of ferroelectric materials, *Appl. Phys. Rev.* **5**, 041101 (2018).
- 6 L. Lv, F. Zhuge, F. Xie, X. Xujing, Z. Qingfu, Z. Nan, H. Yu and Z. Tianyou, Reconfigurable two-dimensional optoelectronic devices enabled by local ferroelectric polarization, *Nat. Commun.* **10**, 3331 (2019).
- 7 A. Haußmann, A. Gemeinhardt, M. Schröder, T. Kämpfe and L. M. Eng, Bottom-up assembly of molecular nanostructures by means of ferroelectric lithography, *Langmuir* **33**, 475 (2017).
- 8 S. V. Kalinin, D. A. Bonnell, T. Alvarez, X. Lei, Z. Hu, J. H. Ferris, Q. Zhang and S. Dunn, Atomic polarization and local reactivity on ferroelectric surfaces: A new route toward complex nanostructures, *Nano Lett.* **2**, 589 (2002).
- 9 S. Dunn and D. Tiwari, Influence of ferroelectricity on the photoelectric effect of  $\text{LiNbO}_3$ , *Appl. Phys. Lett.* **93**, 092905 (2008).
- 10 D. Li and D. A. Bonnell, Ferroelectric lithography, *Ceram. Int.* **34**, 157 (2008).
- 11 S. Dunn, D. Tiwari, P. M. Jones and D. E. Gallardo, Insights into the relationship between inherent materials properties of PZT and photochemistry for the development of nanostructured silver, *J. Mater. Chem.* **17**, 4460 (2007).
- 12 S. Dunn, S. Sharp and S. Burgess, The photochemical growth of silver nanoparticles on semiconductor surfaces — initial nucleation stage, *Nanotechnology* **20**, 115604 (2009).
- 13 J. N. Hanson, B. J. Rodriguez, R. J. Nemanich and A. Gruverman, Fabrication of metallic nanowires on a ferroelectric template via photochemical reaction, *Nanotechnology* **17**, 4946 (2006).
- 14 X. Liu, K. Kitamura, K. Terabe, H. Hatano and N. Ohashi, Photocatalytic nanoparticle deposition on  $\text{LiNbO}_3$  nanodomain patterns via photovoltaic effect, *Appl. Phys. Lett.* **91**, 044101 (2007).
- 15 Y. Sun and R. J. Nemanich, Photoinduced Ag deposition on periodically poled lithium niobate: Wavelength and polarization screening dependence, *J. Appl. Phys.* **109**, 104302 (2011).
- 16 Y. Sun, B. S. Eller and R. J. Nemanich, Photo-induced Ag deposition on periodically poled lithium niobate: Concentration and intensity dependence, *J. Appl. Phys.* **110**, 084303 (2011).
- 17 N. C. Carville, M. Manzo, S. Damm, M. Castiella, L. Collins, D. Denning, S. A. L. Weber, K. Gallo, J. H. Rice and B. J. Rodriguez, Photoreduction of SERS-active metallic nanostructures on chemically patterned ferroelectric crystals, *ACS Nano* **6**, 7373 (2012).
- 18 D. Tiwari and S. Dunn, Photochemical reduction of  $\text{Al}^{3+}$  to  $\text{Al}^0$  over a ferroelectric photocatalyst —  $\text{LiNbO}_3$ , *Mater. Lett.* **79**, 18 (2012).
- 19 X. Liu, H. Hatano, S. Takekawa, F. Ohuchi and K. Kitamura, Patterning of silver nanoparticles on visible light-sensitive Mn-doped lithium niobate photogalvanic crystals, *Appl. Phys. Lett.* **99**, 053102 (2011).
- 20 C. Ke, X. Wang, X. P. Hu, S. N. Zhu and N. Qi, Nanoparticle decoration of ferroelectric domain patterns in  $\text{LiNbO}_3$  crystal, *J. Appl. Phys.* **101**, 064107 (2007).
- 21 S. Habicht, R. J. Nemanich and A. Gruverman, Physical adsorption on ferroelectric surfaces: Photoinduced and thermal effects, *Nanotechnology* **19**, 495303 (2008).
- 22 S. Grilli and P. Ferraro, Dielectrophoretic trapping of suspended particles by selective pyroelectric effect in lithium niobate crystals, *Appl. Phys. Lett.* **92**, 232902 (2008).
- 23 P. Mokry, M. Marvan and J. Fousek, Patterning of dielectric nanoparticles using dielectrophoretic forces generated by ferroelectric polydomain films, *J. Appl. Phys.* **107**, 094104 (2010).

- <sup>24</sup>Z. Zhang, P. Sharma, C. N. Borca, P. A. Dowben and A. Gruverman, Polarization-specific adsorption of organic molecules on ferroelectric LiNbO<sub>3</sub> surfaces, *Appl. Phys. Lett.* **97**, 243702 (2010).
- <sup>25</sup>A. V. Ievlev, A. N. Morozovska, V. Y. Shur and S. V. Kalinin, Ferroelectric switching by the grounded scanning probe microscopy tip, *Phys. Rev. B* **91**, 214109 (2015).
- <sup>26</sup>V. Y. Shur, M. S. Kosobokov, A. V. Makaev, D. K. Kuznetsov, M. S. Nebogatikov, D. S. Chezganov and E. A. Mingaliev, Dimensionality increase of ferroelectric domain shape by pulse laser irradiation, *Acta Mater.* **219**, 117270 (2021).
- <sup>27</sup>X. Li, K. Terabe, H. Hatano and K. Kitamura, Nano-domain engineering in LiNbO<sub>3</sub> by focused ion beam, *J. Appl. Phys.* **44**, L1550 (2005).
- <sup>28</sup>K. Mizuuchi and K. Yamamoto, Domain inversion in LiTaO<sub>3</sub> using an ion beam, *Electron. Lett.* **29**, 2064 (1993).
- <sup>29</sup>X. Li, K. Terabe, H. Hatano, H. Zeng and K. Kitamura, Domain patterning thin crystalline ferroelectric film with focused ion beam for nonlinear photonic integrated circuits, *J. Appl. Phys.* **100**, 106103 (2006).
- <sup>30</sup>D. S. Chezganov, V. Y. Shur, E. O. Vlasov, L. V. Gimadeeva, D. O. Alikin, A. R. Akhmatkhanov, M. A. Chuvakova and V. Y. Mikhailovskii, Influence of the artificial surface dielectric layer on domain patterning by ion beam in MgO-doped lithium niobate single crystals, *Appl. Phys. Lett.* **110**, 082903 (2017).
- <sup>31</sup>D. S. Chezganov, E. O. Vlasov, L. V. Gimadeeva, M. M. Neradovskiy, A. R. Akhmatkhanov, M. A. Chuvakova, D. O. Alikin, H. Tronche, F. Doutre, P. Baldi and V. Y. Shur, Short-period domain patterning by ion beam irradiation in lithium niobate waveguides produced by soft proton exchange, *Opt. Laser Technol.* **158**, 108813 (2023).
- <sup>32</sup>V. Y. Shur, E. V. Pelegova and M. S. Kosobokov, Domain shapes in bulk uniaxial ferroelectrics, *Ferroelectrics* **569**, 251 (2020).
- <sup>33</sup>V. Y. Shur, Correlated nucleation and self-organized kinetics of ferroelectric domains, *Nucleation Theory and Applications*, ed. J. W. P. Schmelzer, 1st edn. (Wiley-VCH, 2005), pp. 178–214.
- <sup>34</sup>I. S. Baturin, A. R. Akhmatkhanov, V. Y. Shur, M. S. Nebogatikov, M. A. Dolbilov and E. A. Rodina, Characterization of bulk screening in single crystals of lithium niobate and lithium tantalate family, *Ferroelectrics* **374**, 1 (2008).
- <sup>35</sup>E. Pashnina, D. Chezganov, A. Slautina, A. Turygin, A. Ushakov, Q. Hu, X. Liu, X. Zhuo, X. Wei and V. Shur, Domain patterning in nonpolar cut PMN–PT by focused ion beam, *J. Adv. Dielectr.* **14**, 2350024 (2024).
- <sup>36</sup>Y. Sheng, A. Best, H.-J. Butt, W. Krolikowski, A. Arie and K. Koynov, Three-dimensional ferroelectric domain visualization by Čerenkov-type second harmonic generation, *Opt. Express* **18**, 16539 (2010).
- <sup>37</sup>M. Ayoub, P. Roedig, K. Koynov, J. Imbrock and C. Denz, Čerenkov-type second-harmonic spectroscopy in random nonlinear photonic structures, *Opt. Express* **21**, 8220 (2013).
- <sup>38</sup>A. A. Esin, A. R. Akhmatkhanov and V. Y. Shur, Superfast domain wall motion in lithium niobate single crystals. Analogy with crystal growth, *Appl. Phys. Lett.* **114**, 192902 (2019).
- <sup>39</sup>V. A. Shikhova, A. S. Slautina, D. S. Chezganov, M. S. Nebogatikov, A. R. Akhmatkhanov, A. P. Turygin, L. I. Ivleva and V. Y. Shur, Formation of broad domain boundary during dot ion beam irradiation in SBN:Ni single crystals, *Ferroelectrics* **592**, 72 (2022).
- <sup>40</sup>L. S. Kokhanchik, E. V. Emelin and V. V. Sirotkin, Morphology features of ferroelectric submicron domains written by e-beam under a metal film in LiNbO<sub>3</sub>, *Coatings* **12**, 1881 (2022).
- <sup>41</sup>L. S. Kokhanchik, E. V. Emelin and V. V. Sirotkin, Large regular arrays with submicron domains written by low-voltage e-beam on  $-Z$  cut of lithium niobate, *Opt. Mater.* **128**, 112405 (2022).
- <sup>42</sup>L. S. Kokhanchik, E. V. Emelin, V. V. Sirotkin and A. A. Svintsov, Deepening of domains at e-beam writing on the  $-Z$  surface of lithium niobate, *J. Phys. D, Appl. Phys.* **55**, 195302 (2022).
- <sup>43</sup>L. S. Kokhanchik, E. V. Emelin, V. V. Sirotkin and A. A. Svintsov, Domain engineering in LiNbO<sub>3</sub> crystals by e-beam and features of spatial distribution of electric field: Experiment and computer simulation, *J. Appl. Phys.* **128**, 144101 (2020).